Am J Physiol Regul Integr Comp Physiol 307: R1–R10, 2014.
First published April 23, 2014; doi:10.1152/ajpregu.00312.2013.

CALL FOR PAPERS | *Integrative and Translational Physiology: Integrative Aspects of Energy Homeostasis and Metabolic Diseases*

Insulin effects on glucose tolerance, hypermetabolic response, and circadian-metabolic protein expression in a rat burn and disuse model

Heather F. Pidcoke,[1] Lisa A. Baer,[2] Xiaowu Wu,[1] Steven E. Wolf,[3] James K. Aden,[1] and Charles E. Wade[2]

[1]*U.S. Army Institute of Surgical Research, Fort Sam Houston, Texas;* [2]*University of Texas Health Science Center at Houston, Houston, Texas; and* [3]*University of Texas Southwestern Medical Center, Dallas, Texas*

Submitted 28 June 2013; accepted in final form 11 March 2014

Pidcoke HF, Baer LA, Wu X, Wolf SE, Aden JK, Wade CE. Insulin effects on glucose tolerance, hypermetabolic response, and circadian-metabolic protein expression in a rat burn and disuse model. *Am J Physiol Regul Integr Comp Physiol* 307: R1–R10, 2014. First published April 23, 2014; doi:10.1152/ajpregu.00312.2013.—Insulin controls hyperglycemia after severe burns, and its use opposes the hypermetabolic response. The underlying molecular mechanisms are poorly understood, and previous research in this area has been limited because of the inadequacy of animal models to mimic the physiological effects seen in humans with burns. Using a recently published rat model that combines both burn and disuse components, we compare the effects of insulin treatment vs. vehicle on glucose tolerance, hypermetabolic response, muscle loss, and circadian-metabolic protein expression after burns. Male Sprague-Dawley rats were assigned to three groups: cage controls ($n = 6$); vehicle-treated burn and hindlimb unloading (VBH; $n = 11$), and insulin-treated burn and hindlimb unloading (IBH; $n = 9$). With the exception of cage controls, rats underwent a 40% total body surface area burn with hindlimb unloading, then IBH rats received 12 days of subcutaneous insulin injections (5 units·kg^{-1}·day^{-1}), and VBH rats received an equivalent dose of vehicle. Glucose tolerance testing was performed on *day 14*, after which blood and tissues were collected for analysis. Body mass loss was attenuated by insulin treatment (VBH = 265 ± 17 g vs. IBH = 283 ± 14 g, $P = 0.016$), and glucose clearance capacity was increased. Soleus and gastrocnemius muscle loss was decreased in the IBH group. Insulin receptor substrate-1, AKT, FOXO-1, caspase-3, and PER1 phosphorylation was altered by injury and disuse, with levels restored by insulin treatment in almost all cases. Insulin treatment after burn and during disuse attenuated the hypermetabolic response, increased glucose clearance, and normalized circadian-metabolic protein expression patterns. Therapies aimed at targeting downstream effectors may provide the beneficial effects of insulin without hypoglycemic risk.

insulin; glucose tolerance; hypermetabolism; circadian rhythm; burn and disuse

HYPERMETABOLISM IS A PROFOUNDLY debilitating consequence of severe burns and is characterized by insulin resistance, hyperglycemia, protein and lipid catabolism, total body protein loss, muscle wasting, elevated temperature, tachycardia, and high-energy requirements that last up to a year after injury (23, 27, 34). Insulin attenuates hyperglycemia after severe burn and decreases the hypermetabolic response, as evidenced by reduced body mass loss, a marker frequently used to track the progression and resolution of the hypermetabolic condition in clinical and research settings (4, 8, 9, 13, 14, 25, 31, 32, 34–36, 52, 63, 64, 69). Associated benefits of treating hyperglycemia include reduced insulin resistance and fewer adverse outcomes (52, 63, 69). The clinical features of the hypermetabolic response to trauma, burns, and disuse are well characterized, as is the relationship to increased protein turnover, inefficient substrate cycling and body mass loss (15, 16, 34, 37, 56, 60). However, underlying molecular mechanisms are not fully understood, and established animal models do not adequately reproduce the combined physiological effects of burns and bed rest that contribute to the profound body mass losses seen in humans (13, 31, 33, 34). A recently published rat model brings together, for the first time, both burn and disuse components from two well-established, highly cited models (71). The resulting losses in total body mass (TBM) and lean body mass (LBM) were similar to those of hypermetabolic, burned humans, and thus can be used as a marker of the hypermetabolic response in this rat model. Hypermetabolism can be inferred if experimental rats lose body mass while the cage control rats gain or maintain their weight (64). It is reasonable to assume that hypermetabolism is the cause of this weight loss, as there is a very large body of literature documenting hypermetabolism and associated body mass loss due to burns both in humans and rats (8, 9, 13, 15, 16, 25, 31, 34, 36, 37, 56, 60, 64). Multiple methods have been used to establish that subjects are hypermetabolic after burns, and that burns result in weight loss (9, 13, 24, 26, 31, 36, 43, 67). Unlike its predecessors, the rat model used here recapitulates the clinical features of body mass loss, demonstrating a higher degree of hypermetabolism, and therefore, it is adequate to study changes in glucose and insulin metabolism in response to large burns and the molecular targets involved (71).

Evidence for integration between the peripheral metabolic pathways and circadian biological rhythms has been growing (3, 17, 38, 51). Diabetic models demonstrate that chronic insulin resistance is linked to alterations in diurnal patterns in glucose and insulin metabolism (6). Many of these same regulators are also involved in atrophy, which may explain complex clinical manifestations after injury (42, 62). To date, these interactions have not been fully described and remain an area of intense investigation. Here, we compare the effects of insulin treatment vs. vehicle on glucose tolerance, hypermeta-

Address for reprint requests and other correspondence: C. E. Wade, Center for Translational Injury Research, Univ. of Texas Health Science Center at Houston, 6431 Fannin St., MSB 5.204, Houston, TX 77030 (e-mail: Charles.E.Wade@uth.tmc.edu).

Report Documentation Page

Form Approved
OMB No. 0704-0188

1. REPORT DATE	2. REPORT TYPE	3. DATES COVERED
01 JUL 2014	**N/A**	**-**

4. TITLE AND SUBTITLE	5a. CONTRACT NUMBER
Insulin effects on glucose tolerance, hypermetabolic response and circadian-metabolic protein expression in a rat burn and disuse model	5b. GRANT NUMBER
	5c. PROGRAM ELEMENT NUMBER
6. AUTHOR(S)	5d. PROJECT NUMBER
	5e. TASK NUMBER
	5f. WORK UNIT NUMBER
7. PERFORMING ORGANIZATION NAME(S) AND ADDRESS(ES) **US Army Institute of Surgical Research, JBSA Fort Sam Houston, Texas**	8. PERFORMING ORGANIZATION REPORT NUMBER
9. SPONSORING/MONITORING AGENCY NAME(S) AND ADDRESS(ES)	10. SPONSOR/MONITOR'S ACRONYM(S)
	11. SPONSOR/MONITOR'S REPORT NUMBER(S)

12. DISTRIBUTION/AVAILABILITY STATEMENT
Approved for public release, distribution unlimited

13. SUPPLEMENTARY NOTES

14. ABSTRACT

15. SUBJECT TERMS

16. SECURITY CLASSIFICATION OF:			17. LIMITATION OF ABSTRACT	18. NUMBER OF PAGES	19a. NAME OF RESPONSIBLE PERSON
a. REPORT	b. ABSTRACT	c. THIS PAGE			
unclassified	**unclassified**	**unclassified**	**UU**	**10**	

Standard Form 298 (Rev. 8-98)
Prescribed by ANSI Std Z39-18

bolic response, and circadian-metabolic protein expression after burns with hindlimb unloading. We hypothesized that the combined injury and disuse model, previously shown to produce a hypermetabolic insult, also results in decreased glucose clearance, increased insulin resistance and muscle loss, and altered circadian-metabolic protein expression. Furthermore, we hypothesized that insulin treatment attenuates the hypermetabolic response, improves glucose tolerance, decreases muscle loss, and normalizes dysregulation in circadian-metabolic protein expression.

METHODS

Regulatory approval was obtained from the U.S. Army Institute for Surgical Research and University of Texas Health Science Center San Antonio Institutional Animal Care and Use Committees. This study was conducted in compliance with the Animal Welfare Act, the implementing Animal Welfare Regulations, and in accordance with the principles of the Guide for the Care and Use of Laboratory Animals. Adult male Sprague-Dawley rats (Charles River Laboratories, Wilmington, MA) were housed in metabolic cages, which allowed for accurate quantification of urine and fecal output. They were given water and a certified diet (Harlan Teklad no. 2018 in powder form) ad libitum. Room temperature was maintained at 76 ± 2°F and 30–80% relative humidity. After a week, the rats weighed ~300 g and were assigned to one of three groups: cage controls group (CC; $n = 6$); vehicle-treated burn and hindlimb unloading (VBH; $n = 11$) group, or the insulin-treated burn and hindlimb unloading (IBH; $n = 9$) group.

We examined the effects of glucose clearance in the burn and hindlimb unloading (BH) injury model on rats and compared findings between animals treated with insulin to those treated with vehicle. Because rat responses to glucose loading vary widely in published literature, the CC group provided baseline reference values for glucose tolerance testing (GTT) in healthy rats from this population. The CC group did not undergo BH procedures or daily injections, but a sham procedure was performed on *day 0*, and GTT was performed just prior to euthanasia. CC results served as reference laboratory, body mass, GTT, and protein expression values for fasted healthy rats subjected to housing in metabolic cages, the stress of sham and GTT procedures, but not injury or treatment.

Scald Procedure

Rats undergoing the BH procedure were weighed and given a preprocedure dose of buprenorphine (0.1 mg/kg) subcutaneously for analgesia. General anesthesia was induced with inhalation of 2–3% isoflurane in 100% oxygen. Animals were initially placed in an induction chamber, then transferred to face mask. Scald procedures were performed according to the method described by Walker and Mason (65). Briefly, dorsal and ventral surfaces were shaved and the animals placed in Plexiglas molds designed to expose 20% of the total body surface area. The dorsal surface was exposed to 100°C water for 10 s, followed by the ventral surface for 2 s, creating a 40% total body surface area injury. Ringer's lactate (20 ml) was injected into the peritoneal space to be absorbed over time for resuscitation (57). Cage-control animals underwent a sham procedure in which anesthesia was administered, and the rats were exposed to water at room temperature.

Postinjury and Hindlimb Unloading Procedures

Following the burn, BH rats were returned to the metabolic cages where they received 2 doses of buprenorphine (0.05 mg/kg sc) for analgesia over the first 24 h. Hindlimb unloading (HU) was performed according to previously published methods (46–48). Briefly, after the animals regained full consciousness from anesthesia and were able to ambulate, their hindquarters were unloaded using a tail traction system. The device prevented weight-bearing on the hindlimbs, while allowing 360° access to the cage environment. The rats were observed for apparent signs of distress and monitored several times a day.

Insulin and Vehicle Administration

Treatment animals were injected daily with subcutaneous long-acting insulin in ~0.04 ± 0.01 ml of saline (5 units·kg^{-1}·day^{-1}, protamine zinc insulin; BCP Veterinary Pharmacy, Houston, Texas) every morning for 12 days per the dose-response curve published by Jeschke and colleagues (35, 39). Vehicle animals received an equivalent volume of saline subcutaneously. Dose volumes varied by 0.01 ml because of the variability in animal weights upon which the doses were calculated.

Physiological Data Collection and Analysis

Behavior, food and water intake, and urine output were assessed and recorded twice daily. TBM was measured daily as a marker of hypermetabolism which has been previously reported in this model (64). Measurements were taken in the hindlimb-unloaded position to avoid weight-bearing. Body temperature was measured daily via laser skin thermometer. Urine corticosterone levels were measured for each 24-h period (2, 64). Plasma analysis of glucose, insulin, C-peptide, and free fatty acids (FFA) was done once on *day 14*. Exogenous insulin was calculated as the result of subtracting C-peptide from total plasma insulin.

Effect of Injury on GTT With and Without Insulin Therapy

The purpose of this experiment was to determine the effect of long-term (14 day) insulin therapy on glucose clearance (GTT) in IBH rats compared with VBH and CC. Insulin was withheld for 24 h, and rats were fasted ~10 h in preparation for the procedure. Glucose tolerance was tested under general anesthesia (1.5–3% isoflurane in 100% oxygen) at *day 7* or *8* for CC rats due to limitations of staff and procedure room availability, and at *day 14* for BH rats (Fig. 1). The purpose of the CC group was to provide a baseline of reference values for GTT values, poststudy laboratory values, normal growth curves in healthy rats in the absence of burn and bedrest, and protein phosphorylation due to the GTT procedure alone. Body mass in the CC group was expected to rise as a result of normal growth but be somewhat attenuated because of the stress of being housed in metabolic cages and handled twice daily. Seven to eight days were considered sufficient to allow such stress effects to equilibrate and to establish the trajectory of growth curves for comparison to those from experimental groups. After measurements of total body mass and baseline blood glucose were taken, a 50% glucose infusion was administered, delivering a 1 g/kg intravenous glucose load. Blood glucose was measured

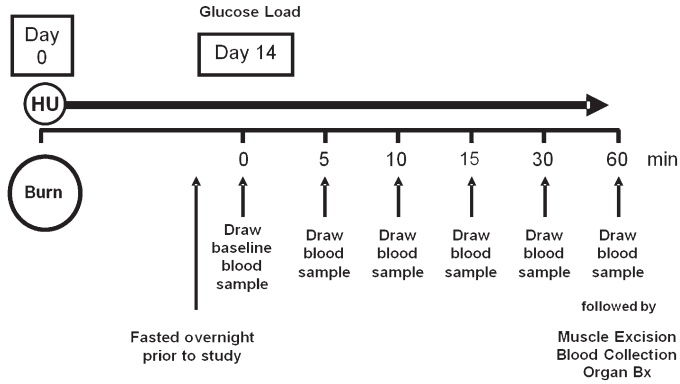

Fig. 1. Glucose tolerance test timeline. Animals were fasted for 10 h prior to testing, which was performed on *day 7* or *8* for cage control rats and *day 14* for insulin and vehicle hindlimb unloaded rats. Sequential blood glucose measurements were taken at times indicated.

at 5, 10, 15, 30, and 60 min (Fig. 1). Rate of glucose clearance was calculated as the total area under the glucose curve and the slope of the GTT natural log regression curve as a measure of disposal rate. The data from the noninsulin-treated VBH rats provided baseline measurements in injured and stressed animals, and data from the cage controls provided baseline measurements in healthy animals.

Euthanasia and Posteuthanasia Procedures

After GTT, animals were euthanized via terminal exsanguination under anesthesia. Organ tissue (heart, liver, spleen, kidney, testes, adrenals, and dorsal fat pads) and skeletal muscle (bilateral tibialis anterior, extensor digitorum longus, plantaris, soleus, and gastrocnemius) were rapidly dissected and weighed. Total muscle was the sum of bilateral muscle weights. Tissue samples were immediately flash frozen with liquid nitrogen, after which lean body mass was determined with dual-emission X-ray absorptiometry scanning (Lunar Prodigy, GE Healthcare, Madison, WI).

Western Blot Analysis

Proteins from the soleus muscle were extracted for Western blot analysis via liquid nitrogen biopulverization in ice-cold 1× commercial cell lysis buffer (Cell Signaling, Danvers, MA) containing a protease inhibitor cocktail (Sigma-Aldrich, St. Louis, MO) and phenylmethylsulfonyl fluoride (Santa Cruz Biotechnology, Santa Cruz, CA) followed by homogenization with a motorized polytetrafluoroethylene pestle. Samples were centrifuged at 14,000 rpm for 10 min at 4°C, and the supernatant was collected for sample analysis. Western blots were run on graduated 4–12% Bis-tris or 4% tris-acetate gels (Invitrogen) and transferred onto nitrocellulose or polyvinylidene fluoride membranes (iBlot Dry Blotting System, Invitrogen). The membranes were incubated with blocking buffer (Odyssey blocking buffer, LI-COR, Lincoln, NE) for an hour, followed by the following primary antibodies: total insulin receptor substrate (IRS-1), AKT, phosphorylated AKT (Ser-473), AMPK-α1, phosphorylated AMPK-α1 (Thr-172), phosphorylated FOXO-1 (Ser-256) (Cell Signaling Technology); phosphorylated IRS-1 (Ser-312), PPARβ, caspase-3, CRY1, CRY2, PER1, PER2, and PER3 (Santa Cruz Biotechnology); phosphorylated IRS-1 (Tyr-612; Abcam, Cambridge, MA). Primary antibodies were incubated at room temperature for 40 min followed by overnight at 4°C. After washing steps were completed, bands were detected and quantified by incubation with fluorescent secondary antibodies (species appropriate IRDye 680 and IRDye 800 secondary antibodies, LI-COR). Membranes were analyzed with a commercial analyzer (Odyssey Infrared Imager, LI-COR Biosciences). Proteins were normalized to β-actin levels and, if in the phosphorylated form, the proteins were normalized to the total abundance. Ratios were calculated for each individual subject and then averaged for the group.

Data Analysis

Group size was determined via power analysis with α set at 0.05 and β set at 0.2. Organ and muscle mass was normalized to body mass and analyzed with commercial software (SigmaPlot 11.2; Systat, San Jose, CA). Significance was set at $P < 0.05$. Normally distributed data were compared using two-way repeated-measures ANOVA and *t*-tests. Values greater than two standard deviations from the mean were excluded. Post hoc analysis was performed with the Holm-Sidak test. Values in the text are group averages ± SD, except as noted.

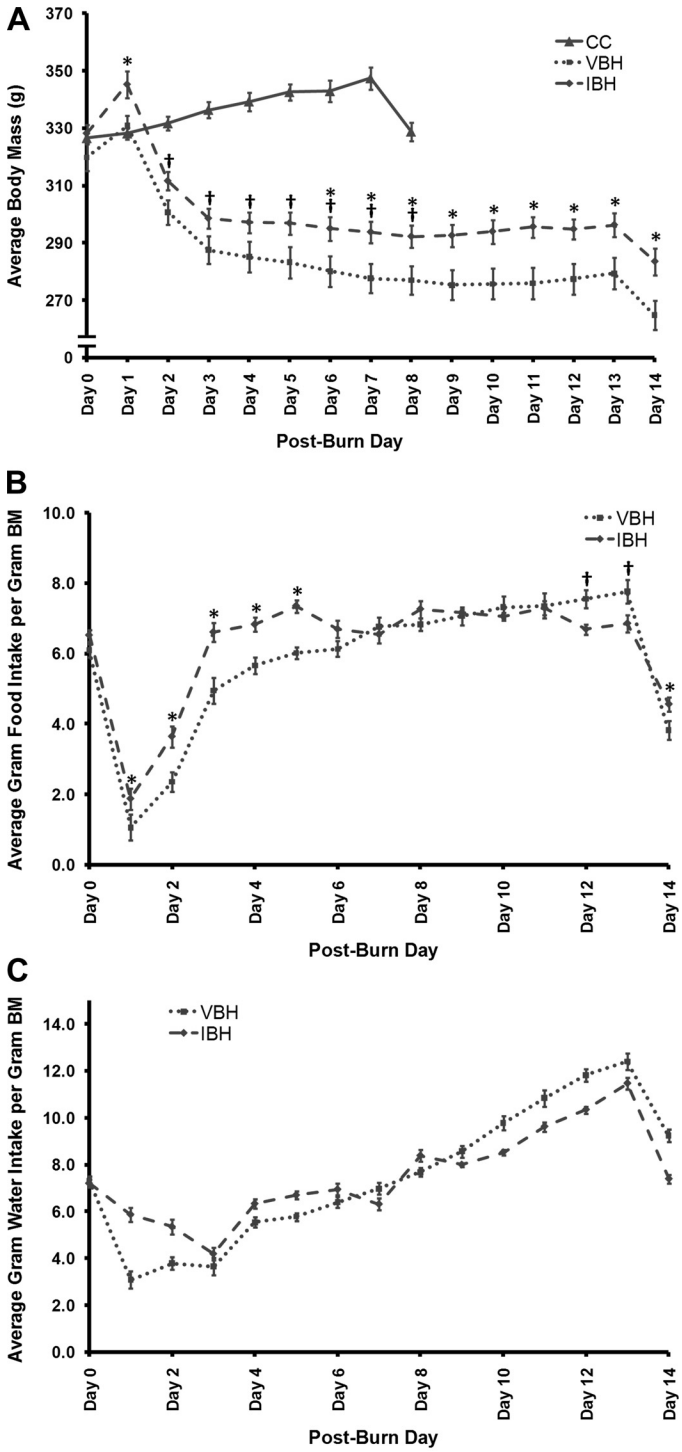

Fig. 2. Average daily body mass (*A*), food intake (*B*), and water intake (*C*). Initial and postburn body mass (BM; g), food intake (g/100 g BM), and water intake (g/100 g BM) were recorded daily until the end of the study on *day 14*. *$P \leq 0.05$, IBH vs. vehicle and hindlimb-unloaded (VBH). †$P \leq 0.001$, insulin-treated burn and hindlimb-unloaded (IBH) vs. cage control (CC).

RESULTS

Effects of Injury and Disuse on Hypermetabolism and Atrophy

There were no significant differences between groups in baseline BM and food intake (Fig. 2). Twenty-four hours after administration, insulin treatment resulted in markedly elevated exogenous plasma insulin levels in both experimental groups ($P = 0.005$; Table 1). The percent contribution of endogenous insulin production was negligible as determined by C-peptide (CC: 0.70 ± 0.26%, $n = 6$; VBH: 1.20 ± 0.50%, $n = 7$; IBH:

Table 1. *Plasma exogenous insulin, plasma free fatty acid, and average daily urinary corticosterone levels in response to injury with and without insulin treatment*

	SD	*P* Value
Exogenous insulin, pg/ml		
CC	606 ± 315	CC vs. VBH, 0.036
VBH	316 ± 70	CC vs. IBH, 0.030
IBH	1910 ± 1257	VBH vs. IBH, 0.005
FFA, nmol/μl		
CC	0.12 ± 0.05	CC vs. VBH, 0.113
VBH	0.08 ± 0.02	CC vs. IBH, 0.718
IBH	0.14 ± 0.09	VBH vs. IBH, 0.172
Corticosterone, ng/day		
CC	494 ± 92	CC vs. VBH, 0.000
VBH	938 ± 460	CC vs. IBH, 0.000
IBH	1117 ± 632	VBH vs. IBH, 0.079

Average values with SD are represented. CC, cage controls; VBH, vehicle-treated; IBH, insulin-treated; FFA, free fatty acid. Post hoc *t*-test *P* values are given for interactions in which the ANOVA was significant.

0.26 ± 0.26%, $n = 8$). Exogenous insulin typically has a suppressive effect on endogenous insulin production, although the phenomenon is likely an indirect effect of lower plasma glucose rather than direct insulin effects (1). Contrary to expectations, however, C-peptide (as a marker of endogenous insulin production) was not suppressed in the IBH group treated with high-dose insulin (CC: 3.9 ± 1.8 ng/ml; VBH: 3.8 ± 1.5 ng/ml; IBH: 2.9 ± 1.1 ng/ml; $P \geq 0.178$). This demonstrates that once-daily subcutaneous dosing resulted in sustained elevations of plasma insulin over the entire period, and these elevations did not result in suppression of endogenous insulin production.

Hypermetabolic effects due to injury and disuse were evident in changes in body mass, urine corticosterone, and the organs involved in stress hormone production. The burn and hindlimb unloading procedure resulted in an initial weight gain in the experimental groups due to administration of intraperitoneal fluid resuscitation (Fig. 2); however, beginning on *day 2*, animals in both experimental groups lost BM over time. Prior to the fasted period, VBH and IBH animals together lost an average of 12.9 ± 3.5% of their BM, in contrast to CC animals, who gained weight over time ($P \leq 0.001$, Fig. 2). All three groups lost ~5% of their body mass when fasted in preparation for the GTTs ($P \geq 0.168$, Fig. 2).

The presence of a hypermetabolic insult was similarly manifested in average daily urine corticosterone levels, a hormone involved in the stress response. Levels were elevated in the experimental groups compared with CC ($P \leq 0.001$; Table 1). In keeping with this finding, the adrenals, involved in stress hormone production, were hypertrophied ($P \leq 0.001$; Table 2). Testicles were atrophied, further evidence of chronically high levels of endogenous steroids ($P \leq 0.001$; Table 2). Interestingly, the heart was hypertrophied in both injury/hindlimb-suspended groups compared with CC ($P \leq 0.007$).

Effect of Insulin Treatment on Hypermetabolism and Atrophy

On *day 6*, insulin treatment attenuated BM loss compared with injury and disuse alone, $P = 0.046$; Fig. 2) and continued through the end of the study (*day 14*: $P = 0.016$; Fig. 2). While both experimental groups lost weight, insulin-treated animals lost a smaller percentage of their BM on average compared with the VBH group (11 ± 2.6% vs. 15 ± 3.3%; $P = 0.012$; Fig. 2). Lean BM decreased in both groups, and differences between experimental groups were not statistically significant (Table 3); however, soleus and gastrocnemius muscle loss was attenuated by insulin treatment. Total food intake over the study period was increased in the IBH group compared with VBH ($P = 0.002$) but not water consumption ($P = 0.986$).

Hypermetabolic changes in some organ weights were attenuated by insulin treatment. The liver was hypertrophied in both the VBH and IBH groups; however; this effect was partially reversed in the insulin cohort ($P \leq 0.001$; Table 2). The meaning of the changes in the spleen and kidney is unclear, particularly as insulin treatment did not affect daily urine output (VBH: 2.9 ± 1.3 ml/100 g BM; IBH: 3.4 ± 2.5 ml/100 g BM, $P = 0.136$). Plasma FFA levels were unchanged by injury/disuse or insulin treatment (Table 1). Rats experienced a significant decrease in fat mass due to hypermetabolism, but the effect was abolished by insulin treatment (CC: 0.88 g/100 g BM; VBH: 0.53 g/100 g BM, $P \leq 0.001$ compared with CC; IBH: 0.82 g/100 g BM, $P \leq 0.001$ compared with VBH, $P = 0.396$ compared with CC).

Effect of Insulin Treatment on Glucose Clearance

Analysis of the GTT curves showed that burn and disuse decreased glucose clearance in the VBH group compared with CC ($P = 0.03$; Fig. 3). Glucose levels rose steeply in both experimental groups after glucose loading (117 to 393 ± 50 vs. 38 to 302 ± 56 g/dl, $P = 0.552$). The area under the GTT curve, a measure of total plasma glucose concentration over time, was lower in the insulin-treated group (VBH: 10,865 ± 2,003 $mg \cdot min^{-1} \cdot dl^{-1}$; IBH: 6,985 ± 1,260 $mg \cdot min^{-1} \cdot dl^{-1}$; $P = 0.003$). The slope of the natural log regression of GTT

Table 2. *Organ mass on day 14*

	CC	VBH	IBH	*P* value IBH to CC	*P* value IBH to VBH
BM	329 ± 6 g	272 ± 12 g	287 ± 11 g	**0.001**	**0.025**
Organ					
Adrenals	0.016 ± 0.002	0.024 ± 0.003	0.024 ± 0.002	**0.000**	0.829
Heart	0.34 ± 0.02	0.38 ± 0.03	0.39 ± 0.04	**0.007**	0.775
Kidney	0.31 ± 0.02	0.38 ± 0.03	0.33 ± 0.02	0.094	**0.001**
Liver	2.65 ± 0.12	3.00 ± 0.13	2.80 ± 0.04	**0.008**	**0.001**
Spleen	0.19 ± 0.03	0.19 ± 0.02	0.15 ± 0.02	**0.002**	**0.000**
Testes	1.06 ± 0.10	0.44 ± 0.05	0.41 ± 0.05	**0.001**	0.343

Average values with SD are represented. Organ mass on *day 14* expressed as g/100 g of *day 14* body mass (BM) in cage controls (CC; $n = 6$), vehicle-treated (VBH; $n = 8$), and insulin-treated rats (IBH; $n = 8$). Post hoc *t*-test *P* values are given for interactions in which the ANOVA was significant. *P* values <0.05 appear in bold.

Table 3. *Muscle mass on day 14*

	CC	VBH	IBH	*P* value IBH to CC	*P* value IBH to VBH
LBM	234 ± 5 g	194 ± 12 g	203 ± 12 g	**0.000**	0.115
Muscle					
Plantaris	0.35 ± 0.01	0.28 ± 0.02	0.29 ± 0.01	**0.000**	0.100
Soleus	0.13 ± 0.01	0.07 ± 0.01	0.08 ± 0.01	**0.000**	**0.025**
Gastrocnemius	1.76 ± 0.06	1.30 ± 0.06	1.37 ± 0.07	**0.000**	**0.028**
Total Muscle	2.98 ± 0.08	2.34 ± 0.10	2.43 ± 0.09	**0.000**	0.059

Average values with SD are represented. Muscle mass on *day 14* expressed as g/100 g of lean body mass (LBM) in CC, VBH, and IBH rats. Post hoc *t*-test *P* values are given for interactions in which the ANOVA was significant. *P* values <0.05 appear in bold.

curves quantifies the rate of glucose clearance, which was over two times faster in the insulin-treated group ($P \leq 0.001$; Fig. 3).

Effect of Insulin on Metabolic and Circadian Protein Expression

IRS-1. Relative abundance of total IRS-1 was decreased in VBH soleus muscle compared with CC ($P = 0.007$; Fig. 4*A*) and in IBH samples ($P = 0.018$). Phosphorylation of IRS-1 at Ser-312 mediates insulin resistance in diabetic models by inhibiting IRS-1 tyrosine phosphorylation and promoting IRS-1 degradation via an mTOR-mediated mechanism (7). After correcting for decreased total IRS-1 levels, we found that Ser-312 was increased in VBH samples compared with CC ($P = 0.034$, Fig. 4*B*). Insulin treatment reversed this effect, and results were similar to those found in the CC group ($P \geq 0.05$).

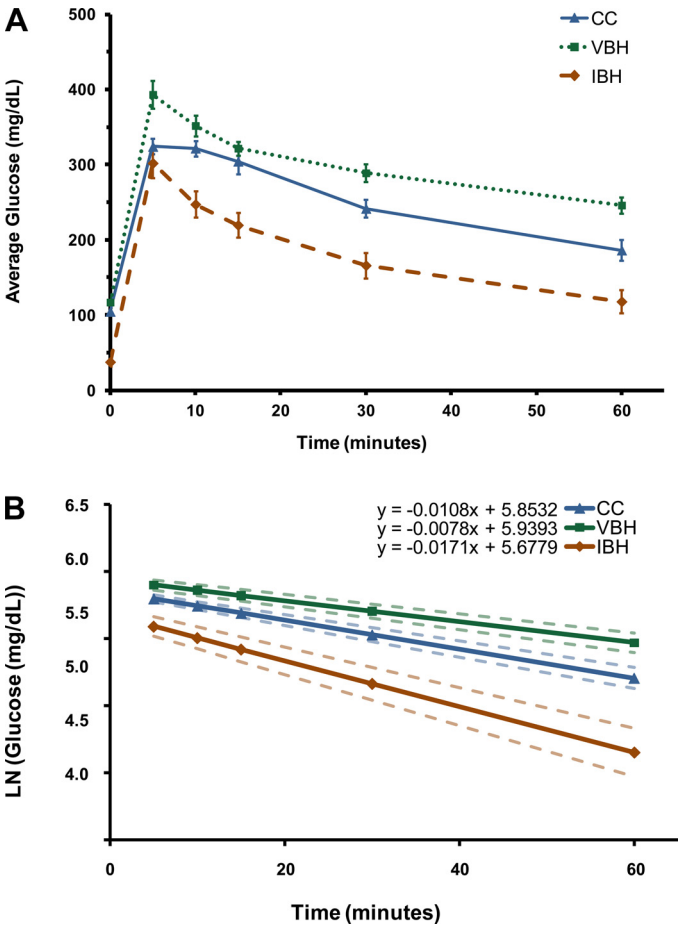

Fig. 3. Glucose tolerance test (*A*) and rate of glucose clearance as a function of the slope of the natural log of glucose values (*B*). $P = 0.03$, slope of VBH vs. CC; $P \leq 0.001$, slope of IBH vs. VBH.

Interestingly, phosphorylation of IRS-1 at Tyr-612 corrected for total IRS-1 abundance was also increased, arguing for a compensatory response to overcome insulin resistance ($P = 0.008$; Fig. 4*C*). Increases in Tyr-612 propagate the IRS-1 activation signal via the p85 subunit of phosphatidylinositol 3-kinase, promoting insulin-mediated effects, such as glucose transport, glycogen and fatty acid synthesis, inhibition of apoptosis, and cellular growth via the AKT pathway (30, 66). Comparing the ratio of stimulatory phosphorylation to inhibitory clarifies the relationship; injury and disuse increased Tyr-612 phosphorylation, but not enough to overcome the concomitant increase in Ser-312 ($P = 0.008$; Fig. 4*D*). Insulin normalized the balance between the two, and the ratio of Tyr-612 to Ser-312 was increased to levels similar to those found in the CC samples ($P = 0.049$, Fig. 4*D*).

AKT. Ser-473-phosphorylated AKT, which activates AKT and propagates the insulin signal downstream via phosphorylation of FOXO-1 and other effectors, was decreased in VBH soleus samples compared with CC ($P = 0.005$, Fig. 5), but insulin treatment reversed this effect (5). Ser-473 phosphorylation is also mediated by mTOR; thus, results are consistent with the above finding that insulin treatment decreases inhibitory phosphorylation, while increasing the state of activation in the insulin pathway (5). This is in contrast to the effect of insulin in diabetic models, in which inhibitory phosphorylation is increased by chronically elevated insulin levels (6, 7, 21).

PPARβ. PPARβ was not different between groups (CC: 0.022 ± 0.015; VBH: 0.022 ± 0.005; IBH: 0.023 ± 0.015; $P \geq 0.891$).

FOXO-1, caspase-3, and AMPK. FOXO-1, caspase-3, and AMPK contribute to apoptosis and have been implicated in atrophy in a variety of models (22, 45, 49, 55). Here, we found no difference between groups in the expression of AMPK phosphorylated at Thr-172, the active form of AMPK, ($P \geq 0.391$, data not shown). Conversely, FOXO-1 and caspase-3 appear to play a role in atrophy due to injury and disuse.

Phosphorylation of FOXO-1 at Ser-256 by AKT excludes FOXO-1 from the nucleus, inhibiting the transcription of mediators involved in apoptosis and cell cycle arrest (22). The net effect of Ser-256 phosphorylation is to promote cell growth and oppose the cellular processes underlying atrophy. Injury and atrophy caused the Ser-256 to total FOXO-1 ratio to decrease relative to cage controls, thereby identifying one pathway to loss of muscle mass in the VBH group ($P = 0.014$; Fig. 6*A*). Insulin treatment reversed this effect; Ser-256 levels in the IBH group increased to baseline levels (IBH vs. VBH:

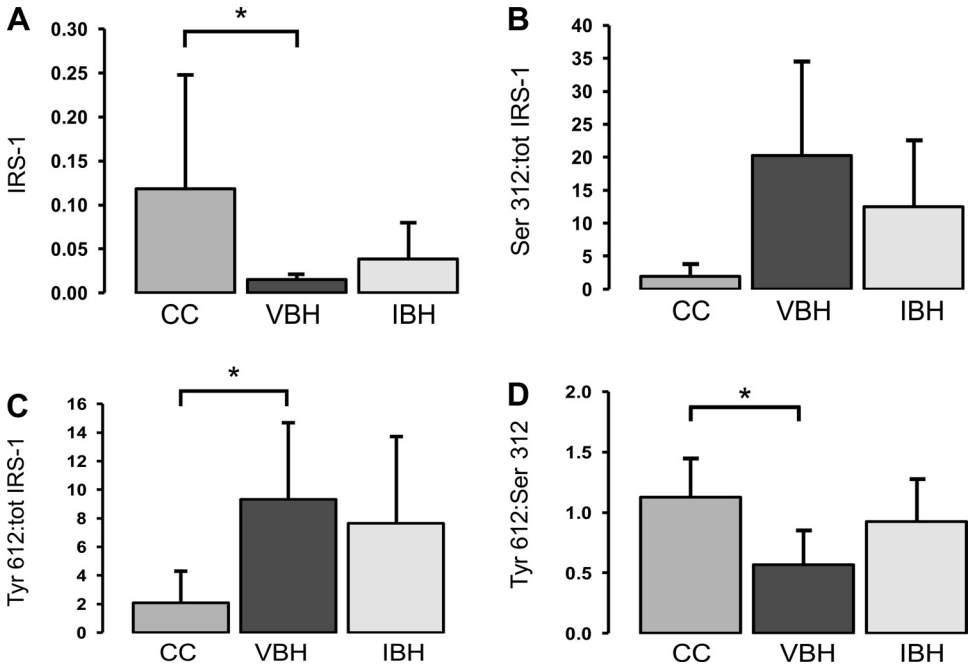

Fig. 4. *A*: change in total IRS-1 due to burn and disuse. The total IRS-1 data from Fig. 4*A* were used to derive the ratios of phosphorylated to total IRS-1 shown in Fig. 4, *B* and *C*. *B*: ratio of IRS-1 phosphorylated at serine-312 to total IRS-1. *C*: ratio of IRS-1 phosphorylated at tyrosine-612 to total IRS-1. *D*: ratio of IRS-1 phosphorylated at tyrosine-612 to IRS-1 phosphorylated at serine-312. Measurements are in arbitrary units and reported as mean ± SD; bars indicate $*P < 0.05$.

$P = 0.001$; IBH vs. CC: P = NS; Fig. 6*A*). Conversely, caspase-3 levels were increased in both experimental groups compared with cage controls ($P \leq 0.046$; Fig. 6*B*), and this effect did not respond to insulin treatment. Taken together, these data show that insulin's effects on FOXO-1 attenuated injury-related soleus muscle loss, while caspase-3 levels were not affected.

CRY1, CRY2, PER1, and PER2. The CRY and PER family of proteins are regulators of the central clock via autofeedback loops, and they are now understood to have a role integrating peripheral circadian rhythms back to the brain (58). CRY1 ($P \geq 0.429$), CRY2 ($P \geq 0.132$), and PER2 ($P \geq 0.268$) expression was not affected by injury, disuse, or insulin treatment.

Conversely, PER1 was altered in the experimental groups. Nuclear PER1 (MW 45) is the active form responsible for inhibition of CLOCK:BMALI transcription; therefore, a high nuclear to cytoplasmic ratio is consistent with decreased circadian oscillations and a loss of central to peripheral integration (58). The nuclear to cytoplasmic PER1 ratio was elevated in the VBH group compared with CC ($P = 0.001$, Fig. 7), while levels in the insulin-treated group were similar to cage controls (IBH vs. CC: $P = 0.418$; IBH vs. VBH: $P = 0.012$; Fig. 7).

DISCUSSION

Severe injury induces a systemic catabolic response characterized by increased energy expenditure; massive loss of lean body mass and decreased bone mineral content (19, 25, 37). Major burn is perhaps the best model for this, as it causes the greatest increase in metabolism (10). Muscle protein synthesis and breakdown are both accelerated, but breakdown accelerates more than synthesis, resulting in a net loss of muscle protein (11, 14). Burn-induced imbalance of protein synthesis and breakdown is sustained continuously from the time of hospital discharge, when wounds are 95% or more healed and persists for 1 yr thereafter, resulting in substantial muscle wasting and atrophy during convalescence (23, 25, 40). Molecular mechanisms and optimal treatments have not been fully characterized.

In a previous study using a modified Walker-Mason model of severe burn injury, acute phase proteins were significantly increased after burn (65); however, they nearly normalized by

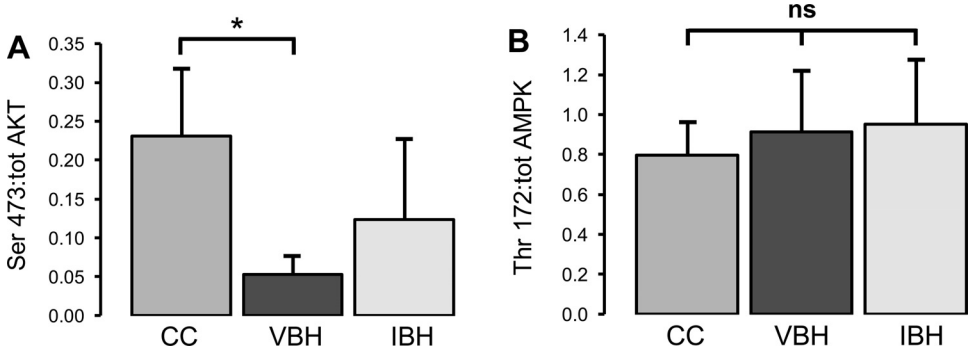

Fig. 5. *A*: ratio of AKT phosphorylated at serine-473 to total AKT. *B*: ratio of Thr-172 to total AMPK. Measurements are in arbitrary units and reported as means ± SD; bars indicate $*P < 0.05$.

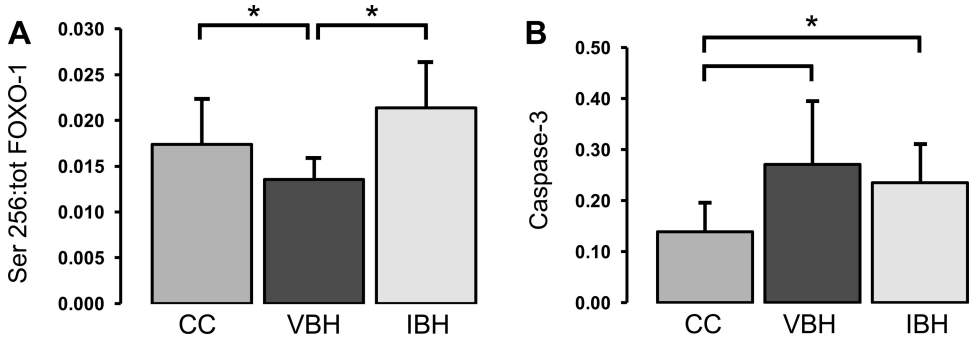

Fig. 6. *A*: ratio of FOXO-1 phosphorylated at serine-256 to total FOXO-1. *B*: change in caspase-3 due to burn and disuse. Measurements are in arbitrary units and reported as means ± SD; bars indicate $*P < 0.05$.

day 14, and this rapid onset of recovery did not adequately mimic the clinical situation seen in severely burned patients (33). Humans display sustained catabolism with continuous loss of muscle mass throughout the hospital stay and for months after complete wound healing (19, 25). One possible explanation is that, since the burned rats in the above study were not restricted in movement after injury, the muscles of the hind-limb received intermittent tension from weight loading, thereby, providing a stimulus for muscle retention after injury. In contrast to rats, patients who have sustained a severe burn usually require long-term bed rest during hospitalization, and have limited mobility once leaving the hospital (37). This inactivity may contribute to the increase in muscle catabolism seen after severe injury and play a role in prolonging the recovery.

Recently, investigators from our laboratory demonstrated that the addition of a disuse component to an established burn model exacerbates hypermetabolism with a cumulative effect that more closely approximates the severity of the human response (2, 71). The model combines a well-published hindlimb-unloading model with a highly cited burn model (46–48, 65, 70). Animals exhibit body mass losses similar to those seen in hypermetabolic humans after burn injury, demonstrating that this model can be used to study the physiological response to large burns (71). HU has been commonly used to study muscle metabolism and the physiological changes due to muscle disuse during the microgravity aspects of space flight and muscle disuse (46, 47, 50, 59). Adding hindlimb unloading and burns to produce a combined model (BH) more closely mimics physiological changes seen in severely burned patients under clinically induced long-term bed rest (71). Burn, in combination with hindlimb unloading results, in a greater loss of body mass than HU or burn alone, and losses continue through postinjury *day 21* (72). BH rats lost both predominantly fast-twitch muscle seen in burns alone and the slow-twitch muscle fibers associated with hindlimb unloading (71). Total body mass was significantly decreased in BH rats at *day 14* compared with burn ambulatory, suggesting that muscle disuse plays an additive role in induction and development of muscle catabolism after burn (71).

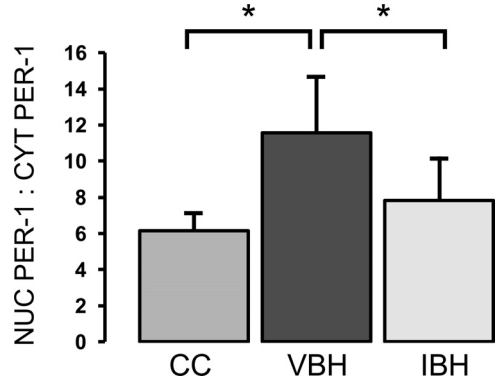

Fig. 7. Ratio of nuclear to cytoplasmic PER-1. Measurements are in arbitrary units and reported as means ± SD; bars indicate $*P < 0.05$.

Prior to the present study, it was not known whether the above model produces the same glucose intolerance seen in hypermetabolic human subjects. Continuous daily insulin therapy is known to prevent lean body mass losses by opposing catabolic processes and has been shown to have antiproteolytic action in burned rats (14, 20, 61), but not enough is known about the physiological changes responsible in order to identify potentially beneficial results or fully characterize the underlying molecular mechanisms.

Our results showed that injury in combination with disuse causes glucose intolerance and increased markers of hypermetabolism in rats, and insulin therapy reduced both glycemic dysregulation and body mass loss. Given these findings, we proceeded to study muscle protein expression and to characterize altered relative abundance of phosphorylated proteins associated with decreased muscle catabolism and improved glucose control after sustained insulin therapy. Because the mediators involved in glycemic and insulin pathways have circadian effects, we wondered whether these proteins would also display altered expression patterns. While our previous data and that of others demonstrated preserved circadian rhythms in critically injured subjects treated with insulin, a recent publication reported the opposite finding (12, 41, 53). Given the mounting evidence for multiple interactions between metabolic and circadian pathways, we investigated expression patterns for IRS-1, AKT, PPARβ, AMPK, FOXO-1, caspase-3, PER2, and CRY1 in two experimental groups, comparing treatment with insulin to vehicle alone.

As expected, this study confirmed that the BH model elicits a hypermetabolic response with both total and lean body mass loss sustained over time (71). Furthermore, significant losses were seen in all muscle groups measured. Corticosterone was elevated in both experimental groups compared with cage controls, a finding that is consistent with the other hypermetabolic effects of the model. Fat mass loss was marked, and the pattern of adrenal hypertrophy in combination with testicular atrophy was indicative of a prolonged stress state. Interestingly, there was no difference in plasma free fatty

acids between groups, and no difference in PPARβ expression, a key regulator of fat metabolism.

Elevated plasma insulin levels drawn more than a day after the final insulin injection confirmed that once-daily subcutaneous insulin dosing successfully resulted in elevated plasma insulin over the entire 24-h period. Glucose tolerance tests were further confirmation of the effects of insulin treatment. VBH rats had decreased glucose clearance and a slower rate of change compared with IBH.

Effects of insulin treatment on total IRS-1 expression were equally interesting. Injury and atrophy had a significantly depressive effect on IRS-1 total protein abundance, but this was partially reversed by treatment with insulin. Differences between cage controls and the insulin-treated group did not meet statistical significance. This effect was seen again in two phosphorylated forms of the protein; Tyr-612 is associated with an activated IRS-1 state, while Ser-312 is an inhibitory phosphorylation site associated with insulin resistance. The abundance ratio of two phosphorylated forms elucidates the relationship; Tyr-612 phosphorylation increases, but not enough to overcome the concomitant increase in Ser-312; thus, the net effect is inhibitory, consistent with the development of insulin resistance after injury. Insulin treatment increased the stimulatory phosphorylation more than it affected the inhibitory, changing the balance between Tyr-612 and Ser-312 IRS-1 phosphorylation. Thus, the relative ratio of stimulatory to inhibitory IRS-1 phosphorylation in the VBH group was statistically different from both the IBH and CC samples, but IBH and CC ratio levels were similar. As with IRS-1 levels, the ratio of phosphorylated (Ser-473) to total AKT provides further evidence of insulin resistance in the VBH group, and insulin treatment normalized the relationship. The rats studied in this model were in the acute "flow" phase after burn and disuse, which, in humans, can last up to a year. Evidence is mounting that the hyperglycemia that is characteristic of this phase may be mediated by insulin resistance. Many burn patients experience a prolonged period of hyperglycemia that lasts well into the rehabilitation phase (1 to 3 yr), as is evidenced by mild to moderate obesity that can follow when the hypermetabolic phase wanes (37). While publications in the 1970s pointed to increased hepatic gluconeogenesis as the culprit (68), recent publications have reported insulin resistance in burned rabbits as measured by euglycemic clamp, as well as degradation of IRS-1 in a murine model (44, 73). These findings suggest, as does our work, that the prevalence of hyperglycemia after burns likely has an insulin resistance component and are further supported by observations of abnormal insulin sensitivity in postburn pediatric patients (18). This phase is usually temporary and eventually resolves for most patients; however, it lasts much longer than the 2-wk duration of these experiments. Our findings suggest that this period of insulin resistance is a product of competing IRS-1 phosphorylation, with inhibitory signaling predominating in the absence of exogenous insulin. Conversely, PPARβ was not altered either by injury and disuse or by insulin treatment.

Results for mediators of atrophy were surprising; AMPK involvement in trauma and disuse has been reported; however; in this study, protein expression of Thr-172, the active form of AMPK, was similar between groups (28). This finding is interesting given the classical role of AMPK in regulating cellular metabolism and as a measure of cellular energy balance. Phosphorylated AMPK was suppressed after the glucose load, which is expected; however, chronic insulin administration should have resulted in up-regulation in the insulin-treated group. This was not seen, however, for reasons that are not clear, and this may be a limitation of the study design in obtaining muscle biopsies after glucose loading. Conversely, caspase-3 was elevated in both experimental groups compared with cage controls and, as expected, was not modulated by insulin. Attenuation of injury- and disuse-related atrophy was primarily mediated via phosphorylation of FOXO-1 at Ser-256, promoting FOXO-1 inactivation, cellular growth, and inhibition of apoptosis; however, it was not sufficient to prevent soleus muscle loss. Ser-256 was significantly decreased in the VBH group, and insulin treatment increased FOXO-1 inactivation, resulting in Ser-256 levels that were similar to that found in the CC groups. This provides a potential mechanism for overcoming the effects of caspase-3 in the setting of injury and disuse; effects in other tissues must be examined.

PER1 was the only circadian modulator with altered expression between groups, a finding that is consistent with its known role of integrating central and peripheral circadian inputs. The elevated ratio of nuclear to cytoplasmic PER1 indicates an increase in negative control, and, therefore, dampened circadian oscillations (58). It was beyond the scope of this study to determine whether such attenuation exists; however; this is an area ripe for further exploration. We have shown in retrospective and animal studies that there is an association between circadian rhythm dampening and adverse outcome (53, 54, 64), and this has also been reported by Palmieri and colleagues (29). This has not been studied in animal models, in part, because eliciting a profound hypermetabolic response has been elusive. The combined burn injury and disuse model more closely resembles clinical scenarios and may allow closer study of the interaction between peripheral and central regulation of glucose in the Burn ICU setting where hyperglycemia is persistent, and zeitgeibers are altered. While such an investigation was beyond the scope of this work, we established that insulin treatment modulated the ratio of nuclear and cytoplasmic PER1, and our findings suggest that insulin-treated rats may have a better outcome in a longer-term study. Future work is needed to further elucidate circadian patterns, gene expression, and the link to outcome.

Our study had limitations; aside from the insufficient number of animals to study diurnal patterns, we elected to forego daily blood sampling to avoid attendant additive stress effects that might obscure study findings and prevented a circadian design. While we measured glucose clearance, there was no true insulin clamp to assess insulin resistance. That said, we were able to show that the glucose tolerance test was performed under clamp-like conditions, because the clearance rate of the subcutaneous insulin dose was prolonged to such an extent that the net change over the 60 min GTT period was presumed to be negligible.

Conclusions

Insulin treatment attenuates hypermetabolism caused by injury in combination with disuse and improves both the rate and quantity of glucose clearance. Therapies aimed at targeting downstream effectors may provide the beneficial effects of insulin in opposing body mass loss and inappropriate protein

breakdown without hypoglycemic risk. Molecular mechanisms responsible for insulin resistance after injury and disuse appear to be inhibitory phosphorylation of IRS-1 that overcomes the stimulatory pathway, an effect that is reversed with insulin administration. Body mass losses are mediated by caspase-3 and FOXO-1, while insulin partially opposes these effects via downstream phosphorylation and inactivation of FOXO-1. PER1 protein expression is altered; further research is needed to elucidate how it interacts with other metabolic proteins and whether this results in altered circadian oscillations.

Perspectives and Significance

This study evaluates, for the first time, the effect of insulin administration on physiological changes, increases in markers of hypermetabolism, and relative abundance of molecular effectors caused by a rat model of severe injury and disuse. This model, when published in 2010, opened up new avenues of investigation. It provides a test bed for examining the effects of potential therapies in the context of a hypermetabolic insults that more closely approximate the severity seen in humans, particularly in the early phases after burn. Here, we demonstrated the feasibility of the strategy by defining important changes induced by insulin administration; however, similar investigations of other mediators known to alter hypermetabolism could be equally fruitful. An exciting area of research involves effects on circadian rhythms, which, because of their function in coordinating central and peripheral changes in metabolism, have the potential to explain some of the global phenomena affecting severely injured populations. This study, while not designed to definitively describe these effects, identified changes in PER1 protein expression, suggesting that this may be a productive area of further research.

ACKNOWLEDGMENTS

The authors thank Dr. Andrew Cap for his support and feedback. The authors also thank the following individuals for their invaluable assistance in the execution of this study: Erica Hagerman, D. Todd Silliman, Krystal Valdez, and Alejandra Mora. The authors would like to thank Angela Beeler for her editorial assistance.

GRANTS

This research was funded by the National Institutes of Health (NIH) (1R01GM063120), the Technologies for Metabolic Monitoring (TMM)/Julia Weaver Fund, a Congressional Directed Program Jointly Managed by the U.S. Army Medical Research and Materiel Command, NIH, NASA, the Juvenile Diabetes Research Foundation, and the Combat Casualty Care Division United States Army Medical Research and Materiel Command. The opinions or assertions contained herein are the private views of the authors and are not to be construed as official or as reflecting the views of the Department of the Army or the Department of Defense.

DISCLOSURES

No conflicts of interest, financial or otherwise, are declared by the authors.

AUTHOR CONTRIBUTIONS

Author contributions: H.F.P., L.A.B., X.W., S.E.W., and C.E.W. conception and design of research; H.F.P., L.A.B., X.W., S.E.W., and C.E.W. performed experiments; H.F.P., L.A.B., J.K.A., and C.E.W. analyzed data; H.F.P., L.A.B., X.W., S.E.W., J.K.A., and C.E.W. interpreted results of experiments; H.F.P. prepared figures; H.F.P., L.A.B., X.W., S.E.W., J.K.A., and C.E.W. drafted manuscript; H.F.P., L.A.B., X.W., S.E.W., J.K.A., and C.E.W. edited and revised manuscript; H.F.P., L.A.B., X.W., S.E.W., J.K.A., and C.E.W. approved final version of manuscript.

REFERENCES

1. **Albareda M, Rigla M, Rodriguez-Espinosa J, Caballero A, Chico A, Cabezas R, Carreras G, Perez A.** Influence of exogenous insulin on C-peptide levels in subjects with type 2 diabetes. *Diabetes Res Clin Pract* 68: 202–206, 2005.
2. **Baer LA, Wu X, Tou JC, Johnson E, Wolf SE, Wade CE.** Contributions of severe burn and disuse to bone structure and strength in rats. *Bone* 52: 644–650, 2013.
3. **Bass J, Takahashi JS.** Circadian integration of metabolism and energetics. *Science* 330: 1349–1354, 2010.
4. **Biolo G, Wolfe RR.** Insulin action on protein metabolism. *Baillieres Clin Endocrinol Metab* 7: 989–1005, 1993.
5. **Case N, Thomas J, Sen B, Styner M, Xie Z, Galior K, Rubin J.** Mechanical regulation of glycogen synthase kinase 3beta (GSK3β) in mesenchymal stem cells is dependent on Akt protein serine 473 phosphorylation via mTORC2 protein. *J Biol Chem* 286: 39450–39456, 2011.
6. **Dallmann R, Viola AU, Tarokh L, Cajochen C, Brown SA.** The human circadian metabolome. *Proc Natl Acad Sci USA* 109: 2625–2629, 2012.
7. **Danielsson A, Nystrom FH, Stralfors P.** Phosphorylation of IRS1 at serine 307 and serine 312 in response to insulin in human adipocytes. *Biochem Biophys Res Commun* 342: 1183–1187, 2006.
8. **Demling RH.** Comparison of the anabolic effects and complications of human growth hormone and the testosterone analog, oxandrolone, after severe burn injury. *Burns* 25: 215–221, 1999.
9. **Demling RH, DeSanti L.** The rate of restoration of body weight after burn injury, using the anabolic agent oxandrolone, is not age dependent. *Burns* 27: 46–51, 2001.
10. **Dickerson RN, Gervasio JM, Riley ML, Murrell JE, Hickerson WL, Kudsk KA, Brown RO.** Accuracy of predictive methods to estimate resting energy expenditure of thermally-injured patients. *JPEN J Parenter Enteral Nutr* 26: 17–29, 2002.
11. **Downey RS, Monafo WW, Karl IE, Matthews DE, Bier DM.** Protein dynamics in skeletal muscle after trauma: local and systemic effects. *Surgery* 99: 265–274, 1986.
12. **Egi M, Bellomo R, Stachowski E, French CJ, Hart G, Stow P.** Circadian rhythm of blood glucose values in critically ill patients. *Crit Care Med* 35: 416–421, 2007.
13. **Fang CH, Li BG, Wang JJ, Fischer JE, Hasselgren PO.** Treatment of burned rats with insulin-like growth factor I inhibits the catabolic response in skeletal muscle. *Am J Physiol Regul Integr Comp Physiol* 275: R1091–R1098, 1998.
14. **Ferrando AA, Chinkes DL, Wolf SE, Matin S, Herndon DN, Wolfe RR.** A submaximal dose of insulin promotes net skeletal muscle protein synthesis in patients with severe burns. *Ann Surg* 229: 11–18, 1999.
15. **Finnerty CC, Mabvuure NT, Ali A, Kozar RA, Herndon DN.** The surgically induced stress response. *JPEN J Parenter Enteral Nutr* 37: 21S–29S, 2013.
16. **Frankenfield D.** Energy expenditure and protein requirements after traumatic injury. *Nutr Clin Pract* 21: 430–437, 2006.
17. **Garaulet M, Madrid JA.** Chronobiological aspects of nutrition, metabolic syndrome and obesity. *Adv Drug Deliv Rev* 62: 967–978, 2010.
18. **Gauglitz GG, Herndon DN, Kulp GA, Meyer WJ, 3rd, Jeschke MG.** Abnormal insulin sensitivity persists up to three years in pediatric patients post-burn. *J Clin Endocrinol Metab* 94: 1656–1664, 2009.
19. **Gore DC, Chinkes DL, Hart DW, Wolf SE, Herndon DN, Sanford AP.** Hyperglycemia exacerbates muscle protein catabolism in burn-injured patients. *Crit Care Med* 30: 2438–2442, 2002.
20. **Gore DC, Wolf SE, Sanford AP, Herndon DN, Wolfe RR.** Extremity hyperinsulinemia stimulates muscle protein synthesis in severely injured patients. *Am J Physiol Endocrinol Metab* 286: E529–E534, 2004.
21. **Greene MW, Sakaue H, Wang L, Alessi DR, Roth RA.** Modulation of insulin-stimulated degradation of human insulin receptor substrate-1 by Serine 312 phosphorylation. *J Biol Chem* 278: 8199–8211, 2003.
22. **Gross DN, Wan M, Birnbaum MJ.** The role of FOXO in the regulation of metabolism. *Curr Diab Rep* 9: 208–214, 2009.
23. **Hart DW, Herndon DN, Klein G, Lee SB, Celis M, Mohan S, Chinkes DL, Wolf SE.** Attenuation of posttraumatic muscle catabolism and osteopenia by long-term growth hormone therapy. *Ann Surg* 233: 827–834, 2001.
24. **Hart DW, Wolf SE, Chinkes DL, Gore DC, Mlcak RP, Beauford RB, Obeng MK, Lal S, Gold WF, Wolfe RR, Herndon DN.** Determinants of skeletal muscle catabolism after severe burn. *Ann Surg* 232: 455–465, 2000.

25. **Hart DW, Wolf SE, Mlcak R, Chinkes DL, Ramzy PI, Obeng MK, Ferrando AA, Wolfe RR, Herndon DN.** Persistence of muscle catabolism after severe burn. *Surgery* 128: 312–319, 2000.
26. **Herndon DN, Hart DW, Wolf SE, Chinkes DL, Wolfe RR.** Reversal of catabolism by beta-blockade after severe burns. *N Engl J Med* 345: 1223–1229, 2001.
27. **Herndon DN, Tompkins RG.** Support of the metabolic response to burn injury. *Lancet* 363: 1895–1902, 2004.
28. **Hilder TL, Baer LA, Fuller PM, Fuller CA, Grindeland RE, Wade CE, Graves LM.** Insulin-independent pathways mediating glucose uptake in hindlimb-suspended skeletal muscle. *J Appl Physiol* 99: 2181–2188, 2005.
29. **Hobson KG, Havel PJ, McMurtry AL, Lawless MB, Palmieri TL, Greenhalgh DD.** Circulating leptin and cortisol after burn injury: loss of diurnal pattern. *J Burn Care Rehabil* 25: 491–499, 2004.
30. **Ito Y, Ariga M, Takahashi S, Takenaka A, Hidaka T, Noguchi T.** Changes in tyrosine phosphorylation of insulin receptor and insulin receptor substrate-1 (IRS-1) and association of p85 of phosphatidylinositol 3-kinase with IRS-1 after feeding in rat liver in vivo. *J Endocrinol* 154: 267–273, 1997.
31. **Izamis ML, Uygun K, Uygun B, Yarmush ML, Berthiaume F.** Effects of burn injury on markers of hypermetabolism in rats. *J Burn Care Res* 30: 993–1001, 2009.
32. **Jahoor F, Shangraw RE, Miyoshi H, Wallfish H, Herndon DN, Wolfe RR.** Role of insulin and glucose oxidation in mediating the protein catabolism of burns and sepsis. *Am J Physiol Endocrinol Metab* 257: E323–E331, 1989.
33. **Jarrar D, Wolf SE, Jeschke MG, Ramirez RJ, DebRoy M, Ogle CK, Papaconstaninou J, Herndon DN.** Growth hormone attenuates the acute-phase response to thermal injury. *Arch Surg* 132: 1171–1175; discussion 1175–1176, 1997.
34. **Jeschke MG, Chinkes DL, Finnerty CC, Kulp G, Suman OE, Norbury WB, Branski LK, Gauglitz GG, Mlcak RP, Herndon DN.** Pathophysiologic response to severe burn injury. *Ann Surg* 248: 387–401, 2008.
35. **Jeschke MG, Einspanier R, Klein D, Jauch KW.** Insulin attenuates the systemic inflammatory response to thermal trauma. *Mol Med* 8: 443–450, 2002.
36. **Jeschke MG, Finnerty CC, Herndon DN, Song J, Boehning D, Tompkins RG, Baker HV, Gauglitz GG.** Severe injury is associated with insulin resistance, endoplasmic reticulum stress response, and unfolded protein response. *Ann Surg* 255: 370–378, 2012.
37. **Jeschke MG, Gauglitz GG, Kulp GA, Finnerty CC, Williams FN, Kraft R, Suman OE, Mlcak RP, Herndon DN.** Long-term persistance of the pathophysiologic response to severe burn injury. *PLoS One* 6: e21245, 2011.
38. **Kino T, Chrousos GP.** Circadian CLOCK-mediated regulation of target-tissue sensitivity to glucocorticoids: implications for cardiometabolic diseases. *Endocr Dev* 20: 116–126, 2011.
39. **Klein D, Schubert T, Horch RE, Jauch KW, Jeschke MG.** Insulin treatment improves hepatic morphology and function through modulation of hepatic signals after severe trauma. *Ann Surg* 240: 340–349, 2004.
40. **Klein GL, Herndon DN, Langman CB, Rutan TC, Young WE, Pembleton G, Nusynowitz M, Barnett JL, Broemeling LD, Sailer DE, McCauley, RL.** Long-term reduction in bone mass after severe burn injury in children. *J Pediatr* 126: 252–256, 1995.
41. **Laha SK, Taylor R, Collin SA, Ogden M, Thomas AN.** Glucose control in critical illness using a web-based insulin dose calculator. *Med Eng Phys* 30: 478–482, 2008.
42. **Lamia KA, Sachdeva UM, DiTacchio L, Williams EC, Alvarez JG, Egan DF, Vasquez DS, Juguilon H, Panda S, Shaw RJ, Thompson CB, Evans RM.** AMPK regulates the circadian clock by cryptochrome phosphorylation and degradation. *Science* 326: 437–440, 2009.
43. **Lang CH, Frost RA, Vary TC.** Thermal injury impairs cardiac protein synthesis and is associated with alterations in translation initiation. *Am J Physiol Regul Integr Comp Physiol* 286: R740–R750, 2004.
44. **Lu XM, Tompkins R, Fischman A.** Burn injury-induced IRS-1 degradation in mouse skeletal muscle. *Int J Burns Trauma* 3: 37–48, 2013.
45. **McClung JM, Kavazis AN, DeRuisseau KC, Falk DJ, Deering MA, Lee Y, Sugiura T, Powers SK.** Caspase-3 regulation of diaphragm myonuclear domain during mechanical ventilation-induced atrophy. *Am J Respir Crit Care Med* 175: 150–159, 2007.
46. **Morey-Holton ER, Globus RK.** Hindlimb unloading of growing rats: a model for predicting skeletal changes during space flight. *Bone* 22: 83S–88S, 1998.
47. **Morey-Holton ER, Globus RK.** Hindlimb unloading rodent model: technical aspects. *J Appl Physiol* 92: 1367–1377, 2002.
48. **Morey ER, Sabelman EE, Turner RT, Baylink DJ.** A new rat model simulating some aspects of space flight. *Physiologist* 22: S23–S24, 1979.
49. **Nakashima K, Yakabe Y.** AMPK activation stimulates myofibrillar protein degradation and expression of atrophy-related ubiquitin ligases by increasing FOXO transcription factors in C2C12 myotubes. *Biosci Biotechnol Biochem* 71: 1650–1656, 2007.
50. **Ohira Y, Yoshinaga T, Nomura T, Kawano F, Ishihara A, Nonaka I, Roy RR, Edgerton VR.** Gravitational unloading effects on muscle fiber size, phenotype and myonuclear number. *Adv Space Res* 30: 777–781, 2002.
51. **Oishi K, Shirai H, Ishida N.** CLOCK is involved in the circadian transactivation of peroxisome-proliferator-activated receptor-α (PPARα) in mice. *Biochem J* 386: 575–581, 2005.
52. **Pham TN, Warren AJ, Phan HH, Molitor F, Greenhalgh DG, Palmieri TL.** Impact of tight glycemic control in severely burned children. *J Trauma* 59: 1148–1154, 2005.
53. **Pidcoke HF, Salinas J, Wanek SM, Concannon M, Loo F, Wirfel KL, Holcomb JB, Wolf SE, Wade CE.** Patterns of exogenous insulin requirement reflect insulin sensitivity changes in trauma. *Am J Surg* 194: 798–803; discussion 803, 2007.
54. **Pidcoke HF, Wanek SM, Rohleder LS, Holcomb JB, Wolf SE, Wade CE.** Glucose variability is associated with high mortality after severe burn. *J Trauma* 67: 990–995, 2009.
55. **Plant PJ, Bain JR, Correa JE, Woo M, Batt J.** Absence of caspase-3 protects against denervation-induced skeletal muscle atrophy. *J Appl Physiol* 107: 224–234, 2009.
56. **Porter C, Herndon DN, Sidossis LS, Borsheim E.** The impact of severe burns on skeletal muscle mitochondrial function. *Burns* 39: 1039–1047, 2013.
57. **Ramzy PI, Wolf SE, Irtun O, Hart DW, Thompson JC, Herndon DN.** Gut epithelial apoptosis after severe burn: effects of gut hypoperfusion. *J Am Coll Surg* 190: 281–287, 2000.
58. **Schmutz I, Ripperger JA, Baeriswyl-Aebischer S, Albrecht U.** The mammalian clock component PERIOD2 coordinates circadian output by interaction with nuclear receptors. *Genes Dev* 24: 345–357, 2010.
59. **Sonnenfeld G.** Use of animal models for space flight physiology studies, with special focus on the immune system. *Gravit Space Biol Bull* 18: 31–35, 2005.
60. **Stapleton RD, Jones N, Heyland DK.** Feeding critically ill patients: what is the optimal amount of energy? *Crit Care Med* 35: S535–S540, 2007.
61. **Thomas SJ, Morimoto K, Herndon DN, Ferrando AA, Wolfe RR, Klein GL, Wolf SE.** The effect of prolonged euglycemic hyperinsulinemia on lean body mass after severe burn. *Surgery* 132: 341–347, 2002.
62. **Um JH, Pendergast JS, Springer DA, Foretz M, Viollet B, Brown A, Kim MK, Yamazaki S, Chung JH.** AMPK regulates circadian rhythms in a tissue- and isoform-specific manner. *PLoS One* 6: e18450, 2011.
63. **van den Berghe G, Wouters P, Weekers F, Verwaest C, Bruyninckx F, Schetz M, Vlasselaers D, Ferdinande P, Lauwers P, Bouillon R.** Intensive insulin therapy in critically ill patients. *N Engl J Med* 345: 1359–1367, 2001.
64. **Wade CE, Baer LA, Wu X, Silliman DT, Walters TJ, Wolf SE.** Severe burn and disuse in the rat independently adversely impact body composition and adipokines. *Crit Care* 17: R225, 2013.
65. **Walker HL, Mason AD Jr.** A standard animal burn. *J Trauma* 8: 1049–1051, 1968.
66. **Wilden PA, Broadway DE.** Effect of phosphotyrosyl-IRS-1 level and insulin receptor tyrosine kinase activity on insulin-stimulated phosphatidylinositol 3, MAP, and S6 kinase activities. *J Cell Physiol* 163: 9–18, 1995.
67. **Williams GJ, Herndon DN.** Modulating the hypermetabolic response to burn injuries. *J Wound Care* 11: 87–89, 2002.
68. **Wilmore DW, Mason AD Jr, Pruitt BA, Jr.** Insulin response to glucose in hypermetabolic burn patients. *Ann Surg* 183: 314–320, 1976.
69. **Wolfe RR.** Glucose metabolism in burn injury: a review. *J Burn Care Rehabil* 6: 408–418, 1985.
70. **Wronski TJ, Morey-Holton ER.** Skeletal response to simulated weightlessness: a comparison of suspension techniques. *Aviat Space Environ Med* 58: 63–68, 1987.
71. **Wu X, Baer LA, Wolf SE, Wade CE, Walters TJ.** The impact of muscle disuse on muscle atrophy in severely burned rats. *J Surg Res* 164: e243–e251, 2010.
72. **Wu X, Wolf SE, Walters TJ.** Muscle contractile properties in severely burned rats. *Burns* 36: 905–911, 2010.
73. **Xu H, Yu YM, Ma H, Carter EA, Fagan S, Tompkins RG, Fischman AJ.** Glucose metabolism during the early "flow phase" after burn injury. *J Surg Res* 179: e83–e90, 2013.